Current Error Space Phasor Based Fixed Band Hysteresis Controller Employed for Shunt Active Power Filter

P. N. Tekwani, Siddharthsingh K. ChauhanB,, Mihir C. ShahC

***Abstract*—Abstract- Current harmonics, which are injected in the utility by nonlinear loads, cause major problems that tend to deteriorate the power quality at the mains. To reduce such harmonics, Active Power Filters (APF) are commonly employed. This paper gives performance analysis of current error space phasor based hysteresis controller for shunt active power filter, which allows precise compensation of harmonic currents produced by nonlinear loads. The controller keeps the current error space phasor within the hexagonal boundary (fixed band) by applying inverter voltage vectors which are adjacent to the output voltage vector (voltage vector at the point of common coupling). Region detection logic enables switching of inverter voltage vector which keeps the current error well within the prescribed hexagonal boundary. The controller has a self-adaptive logic which implements necessary sector changes effectively. Implementation of instantaneous reactive power theory for reference current generation is carried out using DSP TMS320LF2407A.**

***Index Terms*—Active power filters, Current error space phasor, Hexagonal boundary, Hysteresis current controller.**

I. INTRODUCTION

WE Current harmonics produced by non-linear loads are prevalent in today's power systems. Widespread use of power electronic loads (identified harmonic-producing loads) such as high-power diode or thyristor rectifiers, cycloconverters, and arc furnaces while unidentified harmonic-producing load like a low-power diode rectifier used as a utility interface in an electric appliance produces a large amount of harmonic current. The computer power supplies, commercial lighting, rectifier equipment in telecommunication networks, TVs, have resulted in a considerable amount of this harmonic injection. These nonlinear loads, generally draw non-sinusoidal unbalanced currents from ac mains resulting in harmonic injection, reactive power burden, excessive neutral currents and unbalanced loading of ac mains. These harmonics interfere with sensitive electronic equipment and cause unnecessary losses in electrical machinery.

Conventionally, passive filters consisting of tuned L-C filters have been broadly used to suppress harmonics because of low initial cost and high efficiency. However, passive filters have many disadvantages, such as large size, parallel and series resonance that could be created with both load and utility impedances, filtering characteristics strongly affected consequently by the source impedance [1].

P. N. TekwaniA Member IEEE, Siddharthsingh K. ChauhanB,, Mihir C. ShahC A Department of Electrical Engg., Institute of Technology, Nirma University

Shunt active filters were initially proposed in 1971 by Sasaki and Machida [2] as a means of removing current harmonics. When the Active Power Filter (APF) is connected in parallel with the harmonic load, it is called shunt APF [3]. The shunt APF operates as a current source that injects a compensating current in order to cancel the harmonic currents and the reactive fundamental current generally produced by nonlinear non-resistive loads. The shunt APF is thus suitable for nonlinear loads which introduce current harmonics, while for nonlinear loads that produce voltage harmonics, a series APF is used [4]. Application of filter is not only limited to harmonic compensation but it is also used for harmonic damping, harmonic isolation, harmonic termination, reactive-power control for power factor correction and voltage regulation, load balancing, voltage-flicker reduction, and/or their combinations.

Many approaches such as notch filter [5], instantaneous reactive power theory [6], synchronous detection method [7], synchronous d-q frame method [8], flux based control [9] and closed-loop PI controllers [8-9], and sliding mode control [10-11] are used to improve the performance of the APFs. These approaches have become feasible because of the advent of new microelectronic devices such as Digital Signal Processors (DSPs) and availability of fast and accurate Hall effect sensors.

Conventional hysteresis current controller (HCC) scheme used in APFs uses three independent hysteresis controllers one for each phase and hence suffers from lack of coordination between the three individual HCCs, resulting in higher number of switching. In order to decrease the number of switching and in turn the switching frequency, space vector modulation technique is applied to current hysteresis controller which enables the use of zero switching vector along with non zero vectors [12-14].

This paper presents the analysis of a 3- shunt APF, which utilizes current error space phasor based hysteresis controller to compensate load harmonic currents. Performance of the shunt active power filter is analyzed for three methods of reference current generation; (1) generalized instantaneous reactive power theory, (2) synchronous reference frame method, and (3) estimation of reference current by regulating the dc-link voltage. The schemes are rigorously simulated and experimental results of sensed parameters for instantaneous reactive power theory using DSP TMS320LF2407A are also presented.

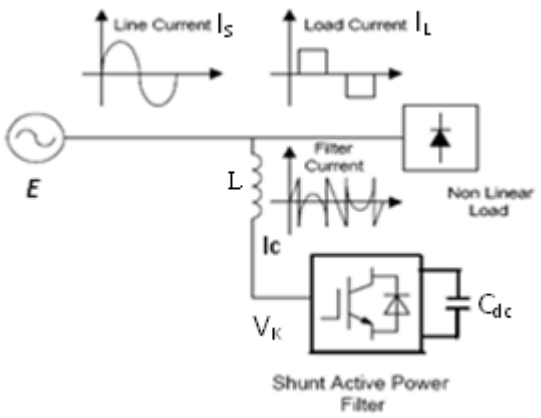

Fig. 1. Shunt active power filter

II. SHUNT ACTIVE POWER FILTER

The shunt active power filter operates as a current source injecting the harmonic components generated by the load but phase shifted by 1800. Moreover, with an appropriate control scheme, the active power filter can also compensate the load power factor. In this way, the power distribution system sees the whole system of nonlinear load and the active power filter as an ideal resistor. The current compensation characteristic of the shunt active power filter is shown in Fig. 1.

III. PRINCIPLE OF SPACE PHASOR BASED CURRENT HYSTERESIS CONTROLLER

The space phasor of the APF current and voltage as well as the voltage at the point of common coupling (PCC) are respectively given by:

$$i_c = \frac{2}{3(i_{ca} + a i_{cb} + a^2 i_{cc})} \quad \ldots (1)$$

$$V_k = \frac{2}{3(V_a + aV_b + a^2 V_c)} \quad \ldots (2)$$

$$E = \frac{2}{3(E_a + aE_b + a^2 E_c)} \quad \ldots (3)$$

Where, $a = e^{-j\frac{2\pi}{3}}$

$$\frac{di_c}{dt} = \frac{1}{L}(V_k - E)$$

Now current error space phasor is

$$\Delta i = i_c^* - i_c \quad \ldots (4)$$

Where i_c^* is reference current space phasor.

Thus rate of change of current error is

$$L\frac{d\Delta i}{dt} = L\frac{di_c^*}{dt} - (V_k - E) \quad \ldots (5)$$

In order to eliminate the current error Δi, the desired output voltage vector V_o^* is obtained from (5) as

$$V_0^* = E + L\frac{di_c^*}{dt} \quad \ldots (6)$$

The direction at which the current error space phasor moves is given by

$$\frac{d\Delta i}{dt} = V_0^* - V_k \quad \ldots (7)$$

Different strategies have been proposed to choose the desired inverter voltage vector to keep the current error space phasor within the boundary [15-16]. The derivative d?i/dt has a vital role in diminishing the number of switching. Choosing a voltage vector Vk, which results in a minimum value of d?i/dt is a necessity to accomplish this task. For the conventional HCC technique, the coordination of the switching does not exist; however, SVM technique causes reduced switching. On the other hand, the utilization of nonzero vectors instead of the zero vector gives steep slope for the current error due to large voltage difference Vo*-VK. Thus, a set of space vectors, two vectors plus the zero vector, is to be applied depending on the position of the desired space voltage vector Vo*.

IV. PROPOSED CURRENT ERROR SPACE PHASOR BASED HYSTERESIS CONTROLLER

In the present hysteresis controller, the current error space phasor is kept within a boundary, by applying one of the three inverter voltage vectors which are adjacent to the voltage vector Vo* so that deviation of current error space phasor is minimum. Fig. 2 shows the inverter voltage vectors and direction of current error space phasor movement for two positions of desired output space voltage vector Vo*. When Vo* is in sector-1(OP); PA, PB and OP' are the directions along which minimum deviation of current error takes place when V1, V2 and V0 are switched respectively. Similar is the case for other sectors. When inverter voltage vector V1 is switched and when Vo* is along OA (which is the boundary between sector-1 and sector-6,) the error space phasor moves along OA. Similarly, for inverter voltage vector V1, the error space phasor will move in the direction of OF when Vo* is along OB (which is the boundary of sector-1 with sector-2). So, for any position of Vo* within sector-1, when vector V1 is switched, the directions in which the error space phasor can move are confined within these two directions. In the same way, for sector- 1, when V2 is switched the current error space phasor can move in any direction, confined within the directions of OC and OB. When zero voltage vector is switched the error space phasor directions are confined within the directions of OD and OE. These three set of directions are shown in Fig.3 (a). This set of directions can be used to define a boundary for the error space phasor, beyond which it should not be allowed to move. For example if the error space phasor moves in a direction parallel to any direction bounded by the directions of OA and OF, it can touch a boundary XZ as shown in Fig. 3(a).This boundary can be decided to be anywhere at a distance 'h' along the jC axis. Similarly, the directions OC and OB define another boundary YX along the jA axis and the directions OD and OE define the third boundary along the jB axis. The same triangular boundary exists for all the odd sectors. In the same manner triangular boundary shown in Fig. 3(b) exists for all the even sectors [16]. Fig. 4 shows the boundary within which the error space phasor can move when Vo* moves through all the sectors.

V. INVERTER VOLTAGE VECTOR SELECTION

This hysteresis controller uses only vectors which are adjacent to Vo*. As mentioned earlier, within a sector, when a particular inverter voltage is switched, it makes the error space phasor to move towards one of the boundaries (Fig. 3(a) and Fig. 3(b)). The inverter voltage vector is continued till the error space phasor reaches another boundary. Once the space phasor hits the boundary, the inverter voltage vector is changed so that error space phasor is brought back within the boundary, and

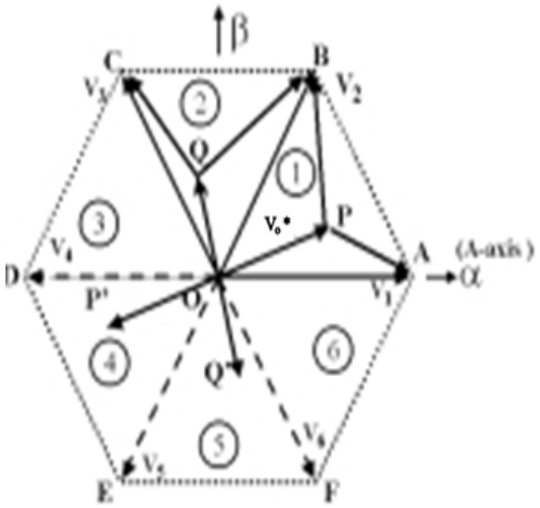

Fig. 2. Output space voltage vector and direction of current error space phasor

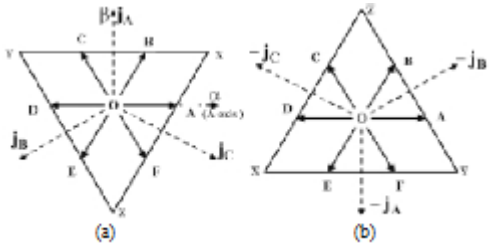

Fig. 3. Boundary of ?i (a) in Sector-1,(b) in Sector-2

moves towards the opposite side of the triangular boundary. The proposed controller divides the triangular boundary to three regions and each of these regions is associated with a suitable inverter voltage vector (depending on the sector) which will take the error space phasor towards the opposite side of the triangular boundary. The triangular boundary of odd sectors is three regions R1, R2 and R3 while that even sectors is divided into , and as shown in Fig. 4 and 5. When the error space phasor hit anywhere in a particular region, a voltage vector is selected so that the error space phasor moves towards the opposite side [16].

For odd sectors the boundaries are placed along the jA, jB, jC axes and for even sectors the boundaries are placed along the - jA, - jB, - jC axes and this would result in the combined boundary as shown in Fig. 6(a). Now, for this triangular boundary, the error space phasor moves to double the distance, along the - jA, - jB, - jC axes in the case of odd sectors and along jA, jB, jC axes for the even sectors. If boundaries are placed along all these axes, for both odd as well as even sectors, it would result in a hexagonal boundary as shown in Fig. 6(b). In the proposed work, the hysteresis controller is implemented with this hexagonal boundary, where along all the six directions (- jA, - jB, - jC, jA, jB, jC), the current error is held always within the hexagonal boundary limits. This hexagonal boundary can be divided into different regions

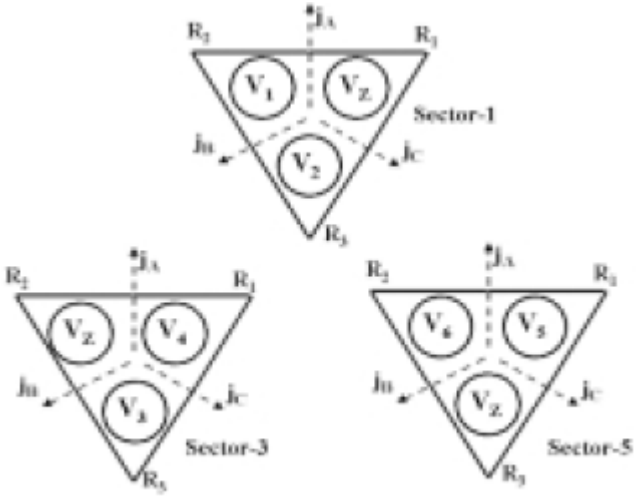

Fig. 4. Regions and corresponding voltage vectors for odd sectors

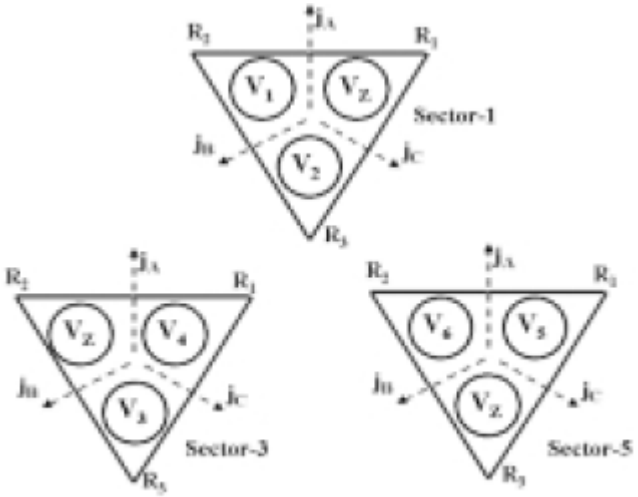

Fig. 5. Regions and corresponding voltage vectors for even sectors

consistent with regions of the triangular boundaries defined in Fig. 4 and 5 [16]. Each region of the hexagonal boundary is associated with an unique vector for each sector which will force the error space phasor to the opposite direction. The different regions and respective inverter voltage vectors to be switched are shown in Table I.

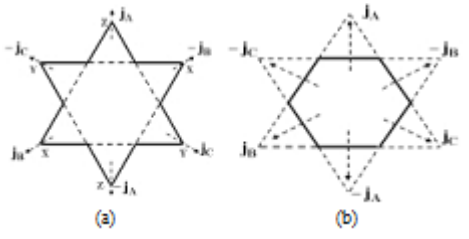

Fig. 6. Boundary of ?i (a) initial, (b) modified

Table I. Voltage vectors to be switched for various regions

Sector	Regions					
	R_1	R_2	R_3	$\overline{R_1}$	$\overline{R_2}$	$\overline{R_3}$
1	V_7	V_1	V_2	-	-	-
2	-	-	-	V_7	V_1	V_7
3	V_6	V_7	V_1	-	-	-
4	-	-	-	V_7	V_6	V_5
5	V_5	V_6	V_7	-	-	-
6	-	-	-	V_1	V_7	V_6

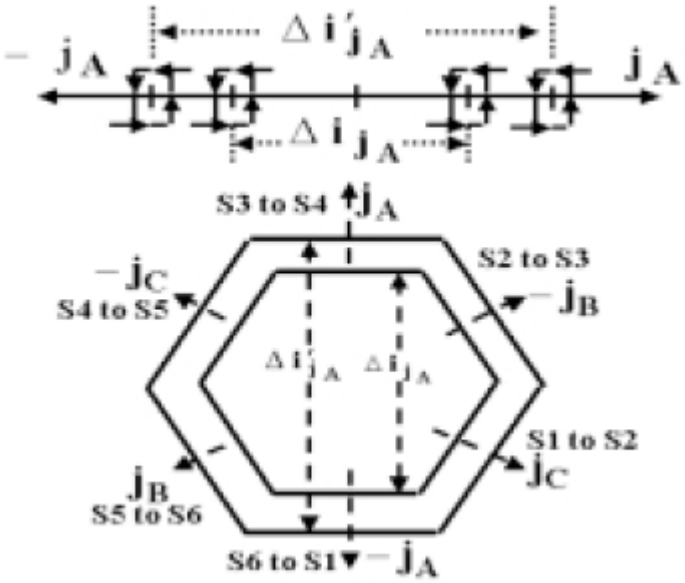

Fig. 7. The outer hysteresis band and the sector changeovers

VI. SECTOR SELECTION LOGIC

The proposed hysteresis controller use s a self-adapting logic to identify the instants at which the Vo* crosses from one sector to another. This sector change is identified with the help of another set of comparators placed a little further than the comparators used for the vector selection. Fig.7 shows the outer hysteresis band placed along all the axes and direction along which sector change takes place [16].

VII. REFERENCE COMPENSATING CURRENT CALCULATION

The shunt active power filter shown in Fig. 1 consists of six semiconductor power switches, a dc-link capacitor as a voltage source and three reactors for limiting the current rate of rise.

1) Instantaneous Reactive Power Theory [6],[17] Based on instantaneous reactive power theory, the compensated currents are derived by measuring line voltage Ea , Eb , Ec load current iLA, iLB, iLC as shown in Fig. 8. First the 3-? line voltages and load currents are transformed into two orthogonal reference vectors E?, E? and i?, i? by Clark's transformation. The instantaneous load active and reactive powers are derived from the transformed voltages and currents. For considering the switching and

$$p = p_{dc} + p_{ac} = E_\alpha i_{l\alpha} + E_\beta i_{L\beta} \quad \text{... (8)}$$

$$q = q_{dc} + q_{ac} = E_\alpha i_{l\beta} - E_\beta i_{L\alpha} \quad \text{... (9)}$$

The compensated currents are calculated as follows:

$$i_{c\alpha}^* = \frac{E_\alpha (p_{ac} + p_{loss}) - E_\beta q}{E_\alpha^2 + E_\beta^2} \quad \text{... (10)}$$

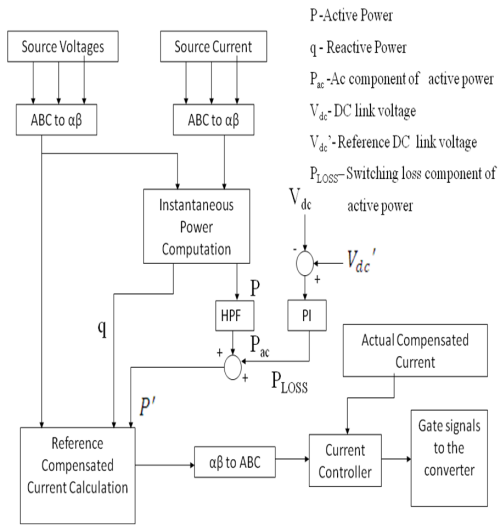

Fig. 8. Control scheme for Instantaneous Reactive Power Theory

conduction loss of the 3-? inverter due to non-ideal solid state devices, Ploss is added to the active power. Therefore compensating currents in three phase form are

$$i_{c\beta}^* = \frac{E_\alpha q + E_\beta (p_{ac} + p_{loss})}{E_\alpha^2 + E_\beta^2} \quad \text{... (11)}$$

$$i_{ca}^* = \sqrt{\frac{2}{3}} i_{c\alpha}^* \quad \text{... (12)}$$

$$i_{cb}^* = \sqrt{\frac{1}{6}} i_{c\alpha}^* + \sqrt{\frac{1}{2}} i_{c\beta}^* \quad \text{... (13)}$$

2) Synchronous Reference Frame method [18-19] The d-q transformation, which changes conventional three rotating phase vectors into direct (d) and quadrature (q) vectors, is proposed in [4].

$$i_{cc}^* = -\sqrt{\frac{1}{6}} i_{c\alpha}^* - \sqrt{\frac{1}{2}} i_{c\beta}^* \quad \text{... (14)}$$

$$i_{Ld} = i_{Ld,ac} + i_{Ld,dc}$$

$$= \sqrt{\frac{2}{3}} \left(i_{La} \cos \omega t + i_{Lb} \cos \omega t - \frac{2\pi}{3} + i_{Lc} \cos \omega t + \frac{2\pi}{3} \right) \quad \text{... (15)}$$

$$i_{Lq} = i_{Lq,ac} + i_{Lq}$$

$$= \sqrt{\frac{2}{3}} \left(-i_{La} \sin \omega t - i_{Lb} \sin \omega t - \frac{2\pi}{3} - i_{Lc} \sin \omega t + \frac{2\pi}{3} \right) \quad \text{... (16)}$$

Where,

ω = angular frequency

For reactive power compensation and current harmonic elimination, the dc offset of iLD is removed by using a high pass filter. The compensated currents ica* , icb* ,

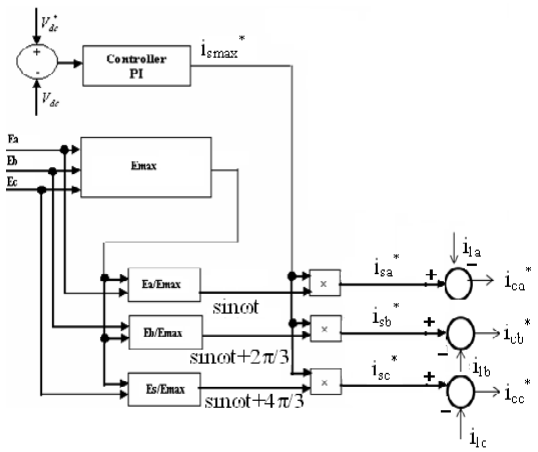

Fig. 9. Control scheme for reference current generation by regulating the dc-link Voltage

icc* can be obtained as follows:

$$i_{ca}^{*} = \sqrt{\frac{2}{3}}\left(i_{Ld,ac}\cos\omega t - i_{Lq}\sin\omega t\right) \quad \ldots (17)$$

$$i_{cb}^{*} = \sqrt{\frac{2}{3}}\left(i_{Ld,ac}\cos\left(\omega t - \frac{2\pi}{3}\right) - i_{Lq}\sin\left(\omega t - \frac{2\pi}{3}\right)\right) \quad \ldots (18)$$

$$i_{cc}^{*} = \sqrt{\frac{2}{3}}\left(i_{Ld,ac}\cos\left(\omega t + \frac{2\pi}{3}\right) - i_{Lq}\sin\left(\omega t + \frac{2\pi}{3}\right)\right) \quad \ldots (19)$$

3) Estimation of Reference Current by Regulating the dc-link Voltage [20-21]:
The basic operation of this method is shown in Fig 9. The estimation of the reference currents from the measured dc bus voltage is the basic idea behind the PI controller based operation of the APF.
The capacitors voltage Vdc is compared with its reference value Vdc* in order to maintain the stored energy in the capacitors constant. The PI controller is applied to regulate the error between the capacitor voltage and its reference. The output of PI controller gives the magnitude ISmax* of the three reference currents, and then this value is multiplied by sinusoidal signals of magnitude equal to the unit in order to obtain the instantaneous supply reference currents isa*, isb*, isc*. These supply reference currents are compared respectively with the nonlinear load currents ila, ilb and ilc and the result of comparison of each phase gives reference compensation currents ica* , icb* , icc*. The result of comparison between this current and the actual compensated current is sent to hysteresis controller in order to generate the switching pulses.

VIII. SIMULATION RESULTS

The space phasor based current hysteresis controlled shunt active power filter is simulated using Matlab7.5 and its tools Power System Blockset and Simulink. Various simulation results are obtained under ideal mains voltage conditions. The

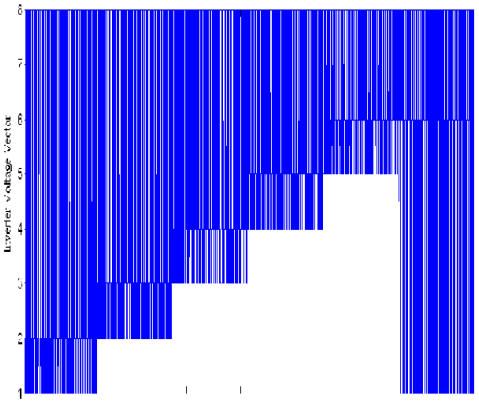

Fig. 10. Inverter voltage vector switched for various sectors

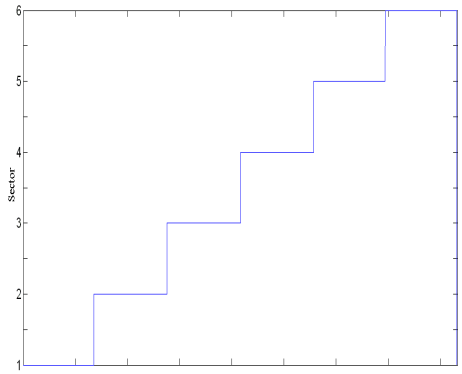

Fig. 11. Sectors of voltage space phasor structure

essential parameters selected for simulation studies are: fundamental frequency = 50 Hz, rectifier load inductance = 1mH, rectifier load resistance = 50 ?, 3-? (Line-Neutral) ac supply voltage = 230 V, APF side inductance = 1mH. Fig. 10(a) and Fig. 10(b) shows the sectors of the hexagonal boundary where in Vo* lies at particular instant and corresponding vectors switched.

1) Instantaneous Reactive Power Theory: Here simulation is carried out using generalized instantaneous reactive power theory. Results are shown in Fig.11 (a) and Fig.11 (b). This active power filter helps to reduce the source current THD from 28.56 (without compensation) to 9.59. Results of Fig.11 (a) clearly depict that controller is fast and accurate enough to enable actual compensating current to track the reference compensating current. Current error space phasor plot is shown in Fig. 11(b). It is seen that current error is restricted well within the hexagonal boundary. Sector change is also clearly visible. Hence the active power filter is able to compensate for any type of change in system. Thus the active power filter can be used in actual system where load change occurs rapidly.
2) Synchronous Reference Frame method: This method for active power filter helps to reduce the source current THD from 28.56 (without compensation) to 4.09.Results are given in Fig.12 (a) and Fig.12 (b). This method is easy to implement. Results clearly depict that controller

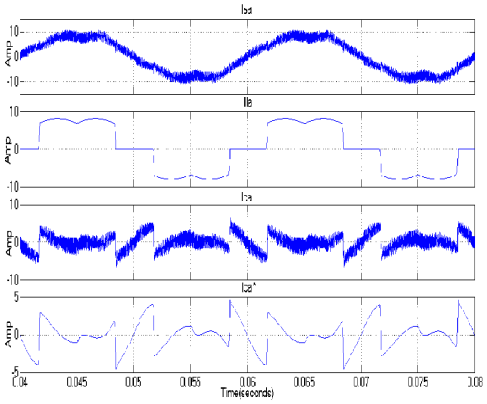

Fig. 12. Instantaneous reactive power theory results for phase A- Source current (Isa); Load current (Ila); Actual compensating current (Ica); Reference compensating current (Ica*)

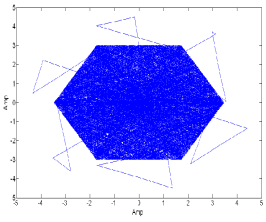

Fig. 13. Synchronous Reference Frame results for phase A- Source current (Isa);Load current (Ila); Actual compensating current (Ica); Referencecompensating current (Ica*)

is fast and accurate enough to track actual compensating current in accordance with reference compensating current. Current error space phasor plot is shown in Fig. 12(b). It is seen that current error is restricted well within the hexagonal boundary. Sector change is also clearly visible.

3) (3) Estimation of Reference Current by Regulating the DC Link Voltage: Dc link capacitor Cdc is taken as 1000F. This method for active power filter helps to reduce the source current THD from 28.56 (without compensation) to 4.02 . Results shown in Fig.13 (a) and Fig.13 (b) clearly depict that controller is fast and accurate enough to track actual compensating current in

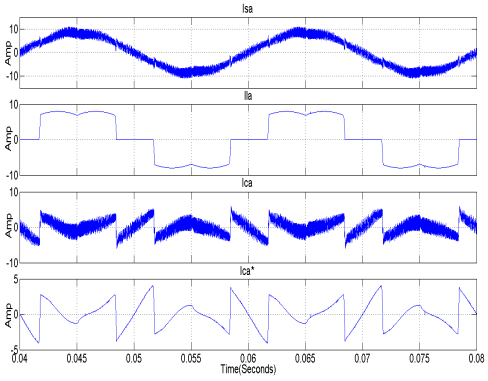

Fig. 14. Current error space phasor

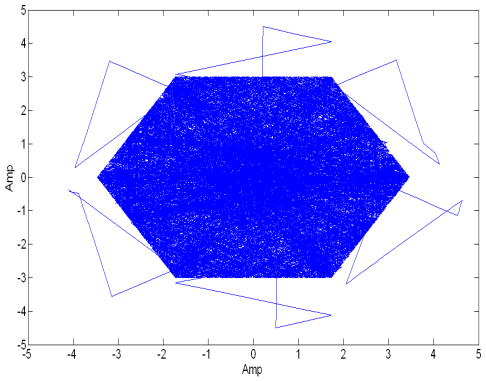

Fig. 15. (a) DC Link Voltage regulation method results for phase A- Source current (Isa); Load current (Ila); Actual compensating current (Ica); Reference compensating current (Ica*)

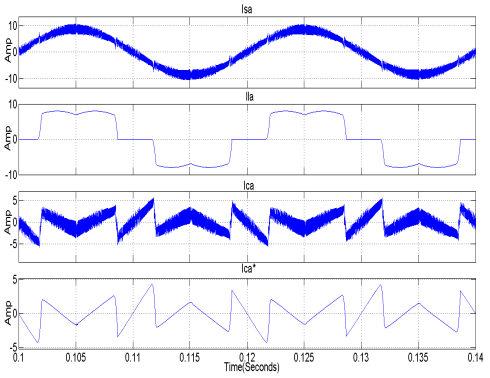

Fig. 16. Current error space phasor

accordance with reference compensating current. Current error space phasor plot is shown in Fig. 13(b). It is seen that current error is restricted well within the hexagonal boundary. Sector change is also clearly visible

IX. EXPERIMENTAL RESULTS

To validate the performance, a prototype test bed has been built for 415V, three phase utility. The major parameters include: dc bus voltage: 110V, dc bus capacitor size: 1000uF. The whole control algorithm i.e. The Instantaneous Reactive Power Theory is being implemented using DSP TMS320LF2407

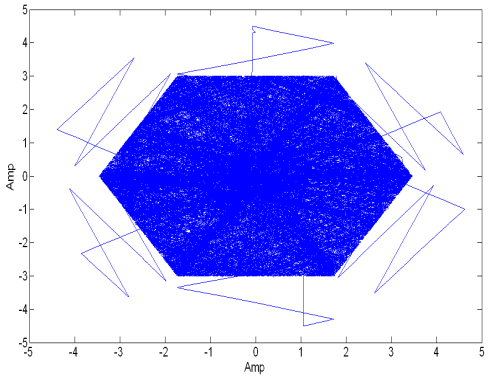

Fig. 17. Current error space phasor

which is a 16-bit fixed point processor with a 40 MHz clock frequency. The load is emulated by a three phase diode bridge rectifier with a resistance of 100 ? and a smoothing capacitor. Fig 14 shows the nonlinear load current and line voltage at 110 V dc-link. Experimental results for Clarke's transformation using DSP are shown in Fig. 15(a) and 15(b).

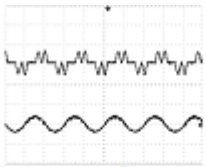

Fig. 14 Nonlinear load current and Line voltage [Scale : - X axis – 10.0ms, Y axis: - 1.00V/div]

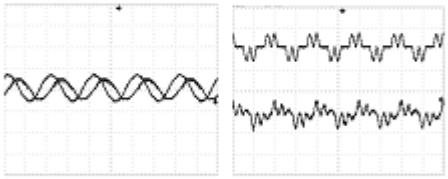

(a) (b)

Fig. 15 (a) Clarke's Transformation of line voltage [X axis – 10.0ms, Y axis: - 1.00V/div], (b) Clarke's Transformation of load current [Scale : - X axis – 10.0ms, Y axis: - 1.00V/div]

X. CONCLUSION

A simplified approach of applying space phasor based current error hysteresis controller to shunt active power filter is presented in this paper. Controller is tested for three types of reference current generation techniques of shunt active power filter to depict its performance. The simulations based on Matlab/Simulink software show that response of controller is good and is able to maintain the current error within desirable hexagonal boundary. Line current is having good THD and low harmonics. Experimental results of instantaneous reactive power theory using DSP TMS320LF2407A are also presented.

REFERENCES

[1] H. Akagi, "New Trends in Active Filters for Power Conditioning", IEEE Transactions on Industry Applications, Vol. 32, No. 6, Nov.-Dec. 1994, pp. 1312-1322

[2] H. Sasaki and T. Machida, "A New Method to Eliminate AC Harmonic Currents by Magnetic Flux Compensation", IEEE Trans. Power Appl. Syst., Vol. PAS-90, No. 5, pp. 2009-2019,1971.

[3] B. Singh, K. Al-Haddad and A. Chandra, "A Review of Active Filters for Power Quality Improvement", IEEE Transactions on Industrial Electronics, Vol. 46, No. 5, Oct. 1999, pp. 960-971.

[4] Z. Wang, Q. Wang, W. Yao and J. Liu, "A Series Active Power Filter Adopting Hybrid Control Approach", Power Electronics, IEEE Trans. on, Volume: 16 Issue: 3, May 2001, Page(s): 301-310.

[5] G. Kamath, N. Mohan, V.D. Albertson, "Hardware implementation of a novel reduced rating active filter for threephase, four-wire loads", IEEE-APEC Conf., pp 984-989, 1995.

[6] T. Furuhashi, S. Okuma, Y. Uchikawa, "A study on the theory of instantaneous reactive power", IEEE Trans. Ind. Electron Vol. 37, no 1, pp 86-90, 1990

[7] C.L. Chen, C.E. Lin, C.L. Huang, "An active filter for unbalanced three-phase system using synchronous detection method", IEEE-PESC Conf., pp 1451-1455, 1994.

[8] S. Bhattachrya, D. Divan, "Synchronous Frame based controller implementation for a hybrid series active filter systems", IEEEIAS Annual Meeting, pp 2531-2540, 1995.

[9] S. Bhattacharya, A. Veltman, D.M. Divan, R.D. Lorenz, "Flux based active filter controller", IEEE-IAS Annual Meeting, pp 2483-2491, 1995.

[10] Z. Radulovic, A. Sabanovic, "Active filter control using a sliding mode approach, IEEE-PESC Conf. , pp 177-182, 1994.

[11] S. Saetieo, R. Devaraj, D.A. Torrey, "The design and implementation of a three-phase active power filter based on sliding mode control, IEEE Trans. Ind. Appl. vol. 31, no.5, pp 993-1000, 1995

[12] M.P.Kazamierkowski, W.sulkowski and M.A.Dzieniokowski , "Novel space vector based current controllers for PWM inverters," IEEE Trans., Power Electronics, Vol.6, No.1, pp.158-166, January 1991.

[13] C.T.Pan and T.Y.Chang, "An improved hysteresis current controller for reducing switching frequency," IEEE Trans., Power Electronics, Vol.9, No.1, pp. 97-104, 1994.

[14] T.Y.Chang, K.L.Lo and C.T.Pan, "A novel vector control hysteresis current controller for induction motor drives," IEEE Trans., Energy conversion, Vol.9, No.2, June 1994.

[15] B. H. Kwon, T. W. Kim and J. H. Youm, "Novel SVM based hysteresis current controller", IEEE Trans. Power. Electronics, Vol.13, No.2, pp 297-307, March 1998.

[16] Baiju, M.R., Mohapatra, K.K., Kanchan, R.S., Tekwani, P.N., and Gopakumar, K.: 'A space phasor based self adaptive current hysteresis controller using adjacent inverter voltage vectors with smooth transition to six step operation for a three phase voltage source inverter', EPE J., 2005, 15, (1), pp. 36-47

[17] S. Bhattachrya, D. Divan, "Synchronous Frame based controller implementation for a hybrid series active filter systems", IEEEIAS Annual Meeting, pp 2531-2540, 1995.

[18] Murat Kale and Engin Ozdemir "A novel adaptive hysteresis band current controller for shunt active power filter" , Electric Power System Research, vol.73, February 2005

[19] Ambrish Chandra, B.Singh, B.N. Singh and K.Al-Haddad "An improved control algorithm of shunt active filter for voltage regulation, harmonic elimination, power-factor correction, and balancing of nonlinear Loads" IEEE Transaction on Industrial Applications, vol.15, no.3, pp.495-507, May 2000.

[20] E.E. EL-Kholy, A. EL-Sabbe , A. El-Hefnawy and Hamdy M. Mharous "Three-phase active power filter based on current controlled voltage source inverter" , International Journal of Electrical Power and Energy Systems, vol.28, Oct. 2006.

[21] F. Z. Peng. and J. Lai. "Generalized Instantaneous Reactive Power Theor' for Three-Phase Power Systems."' IEEE Transactions on Instrumentation anid Measurement. Vol. 45. No. 1, pp.293-297, Februarv 1996

Dr.P.N.Tekwani received B.E. degree in Power Electronics (Gold Medalist, University First) from Saurashtra University, India, in 1995, the M.E. degree in Electrical Engineering (First Rank), with specialization in Industrial Electronics from the M.S. University, Vadodara, in 2000, and the Ph.D. degree (Best Thesis Award) from CEDT, Indian Institute of Science, Bangalore, India in 2006. He was with Amtech Electronics, Gandhinagar, from 1995 to 1996. From 1996 to 2001, he was with Electrical Research and Development Association (ERDA), Vadodara, and since 2001 he has been a Member of the Faculty at the Institute of Technology, Nirma University, Ahmedabad, India. Presently he is a Professor of Electrical Engineering and Coordinator of PG Electrical Engg. (PEMD) Programme. Dr. Tekwani received IEI Young Engineer Award 2010-2011, ISTE-SGSITS National Award for Best Research by Young Teacher-2009, Young Engineer Award-2008 from INAE, and Best paper awards several times at various National and International conferences. He is the Member of ISTE, Society of Power Engineers (I), and IE(I). Dr. Tekwani has more than 50 research publications to his credit and his area of interest is power electronics, power quality, power supplies, and drives.

Siddharthsingh K. Chauhan received his B.E. degree in Electrical Engineering from Gujarat University, Ahmedabad, India in 2003, M.E. degree in Electrical Engineering from Sardar Patel University, V.V.Nagar, India, in 2005 and currently pursuing Ph.D. in Electrical Engineering at the Institute of Technology, Nirma University, Ahmedabad, India. His current research interests include areas of Power Quality, Power Electronics and Active Power filters.

Mihir C. Shah received his B.E. degree in Instrumentation Engineering from University of Mumbai, India in 2009 and currently pursuing M.Tech. in Electrical Engineering (Power Electronics, Machines and Drives) at the Institute of Technology, Nirma University, Ahmedabad, India. His current research interests include areas of Power Quality, DSP applications in Power Electronics and Electrical Drives